J Solid State Electrochem (2003) 7: 177–182
DOI 10.1007/s10008-002-0283-6

ORIGINAL PAPER

J.O. Zerbino · L.M. Gassa

Electrochemical impedance spectroscopy study of cuprous oxide films formed on copper: effect of pH and sulfate and carbonate ions

Received: 23 November 2001 / Accepted: 11 March 2002 / Published online: 23 August 2002

Abstract The semiconducting properties of anodic passive films formed potentiostatically on polycrystalline copper in aqueous borax solutions were studied using electrochemical impedance spectroscopy, photocurrent spectroscopy and ellipsometric measurements. The semiconducting nature of the cuprous passive layer was analysed as a function of pH ($9.2 > pH > 7.4$), electrode potential and with the addition of 3.5 mM Na_2CO_3 and 8 mM Na_2SO_4. The different growth conditions change the compactness and the defect or excess of cations accumulated in the compact inner cuprous layer, leading to different semiconducting properties.

Keywords Copper oxide · Electrochemical impedance spectroscopy · Ellipsometry · Photocurrent spectroscopy · Semiconducting properties

Introduction

Artificial patinas are commonly applied to protect copper from further corrosion. The electrode potential, the presence of different ions in the electrolyte and the effect of ultraviolet light were found to modify the rate of growth and structure of the patina [1, 2]. The patina can be described as a complex structure with a Cu_2O inner layer and an outer Cu(II) oxide or hydroxide layer. Although the corrosion behaviour depends on the presence of both layers, the inner compact layer principally determines the passivity, the open circuit potential and the photoelectrochemical response [3, 4, 5, 6, 7, 8]. In previous works the passive films have been studied in borax for potentials that are cathodic with respect to the bulk formation of CuO. The structure of the cuprous oxide layer formed on the metal was analysed using cyclic voltammetry, photocurrent spectroscopy, reflectance and ellipsometry. It was observed that sulfate concentrations higher than 6 mM promoted the formation of more compact layers [4, 7].

Likewise, it has also been reported [4, 5, 6, 7, 8, 9, 10, 11] that Cu_2O exhibits either p-type or n-type semiconductor properties, depending on the method of preparation and the chemical composition of the aqueous medium in which the oxide layers is formed. On the other hand, the presence of Cu(II) adsorbed on the Cu_2O/electrolyte interface has been reported, as well as the formation of a $CuO_{0.67}$ phase at cathodic potentials not far from the Cu_2O/CuO redox potential (670 mV, 747 mV) [4, 12]. $CuO_{0.67}$ yields the same diffraction lines as those of Cu_2O and only those lines. These processes may be related to a limiting thickness of the Cu_2O layer observed prior to the Cu(II) dissolution.

The present paper is devoted to analysis of the electronic characteristics and structure of the films formed on copper in borate solutions at different pH values using electrochemical impedance spectroscopy (EIS). The influence of the addition of carbonate ions as well as sulfate ions on the structure of the copper layers, and on their semiconducting behaviour, will be presented and discussed. The comparison of the space-charge capacitance obtained under the different growth conditions enables us to gain a deeper insight into the different processes involved in this complex interface.

Experimental

The experimental set-up has been described previously [4, 5, 6, 7, 13]. Polycrystalline copper rods (99.99% purity, area 0.4 cm^2) were used as working electrodes. Prior to each experiment, the electrodes were mechanically polished to a mirror finish with 0.3 and 0.05 μm alumina. The counter electrode was a cylindrical platinum sheet placed around the working electrode. A Pt/H_2 electrode, coupled to a Luggin-Haber capillary tip, was used as the reference electrode for all potential measurements.

The experiments were performed at room temperature and under bubbling of nitrogen in the borate buffer solutions (A)

J.O. Zerbino (✉) · L.M. Gassa
Instituto de Investigaciones Fisicoquímicas
Teóricas y Aplicadas (INIFTA), C.C. 16, Suc. 4,
1900 La Plata, Argentina
E-mail: jzerbino@inifta.unlp.edu.ar
Fax: +54-221-25-4642

0.075 M $Na_2B_2O_7$ + 0.15 M H_3BO_3 (pH 9.2) and (B) 0.005 M $Na_2B_4O_7$ + 0.18 M H_3BO_3 (pH 7.4), with and without the addition of either 8 mM Na_2SO_4 or 3.5 mM Na_2CO_3.

Ellipsometry was used to illuminate the sample with monochromatic light in the wavelength range 400 nm < λ < 700 nm and with an incident angle of 70°. The ellipsometric parameters were obtained after 5 min of holding the potential at E_c = –0.312 V vs. RHE. Then the amplitude, δi, of the photocurrent was recorded as a function of the potential, E, and the time. The potential was scanned from E_c up to E_a at a sweep rate v = 0.5 mV s^{-1} followed by a potential holding at E_a during a time τ. During the E_a holding, the ellipsometric parameters Δ and ψ were recorded simultaneously with δi as a function of τ. A cathodic scan from E_a up to E_c was subsequently performed.

In the photocurrent measurements an EG&G PAR 5210 lock-in analyser and a chopper set at a frequency of 20 Hz were used. The whole area of the electrode was illuminated with a mercury lamp (100 W, 600 B General Electric H100A 4-T). The light passed through a filter (Corning Glass Works 7.54, selecting λ in the region 240 nm < λ < 400 nm, λ = 320 nm) and a quartz window placed in front of the electrode at a distance of 13 mm.

Electrochemical impedance measurements in the potential range 0.35 V ≤ E ≤ 0.685 V were carried out using a Zahner Im6d. Before each experiment the polished electrode was cathodized at E_c = –0.32 V, scanned at v = 0.5 mV s^{-1} up to E_a and pre-anodized at E_a for 1 h to establish a quasi-steady state corresponding to almost constant thickness and passive layer composition according to the fixed E_a value. The impedance measurements in the 65 kHz ≤ f ≤ 1 mHz frequency range were started at this upper E_a potential limit and proceeded in steps of 0.02 V towards lower E potentials within the passive region.

Results and discussion

Optical data

Figure 1 shows the simultaneous current, i, and photocurrent, δi, detection during the formation and reduction of the Cu_2O layer; when the anodic scan ends the potential is held either at E_a = 0.645 V or E_a = 0.685 V for a time τ = 1 h. These potentials are closed to the open circuit potential spontaneously obtained when freshly polished copper electrodes are immersed in aqueous solution. The upper part of the figure shows a current/potential voltammogram similar to those reported in previous experiments [4, 5, 6, 7]. The i vs. E plot shows above E = 0.50 V as the current increases. This potential value agrees with the thermodynamic potential of 0.47 V, corresponding to the Cu/Cu_2O couple [5]. When the potential reaches E_a, i begins to decrease during the time τ. At 0.24 V in the same i vs. E plot can be observed the cathodic peak corresponding to the oxide layer reduction.

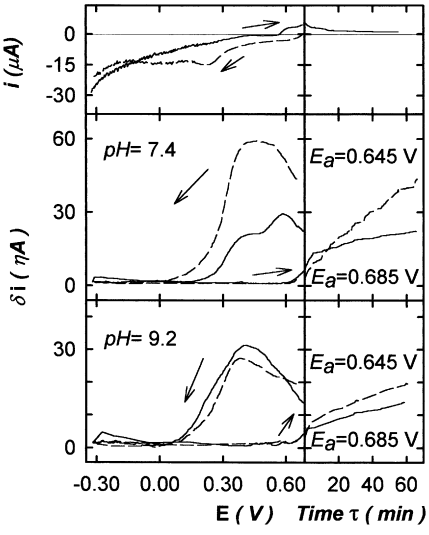

Fig. 1 Photocurrent δi corresponding to the first potential scan at v = 0.5 mV s^{-1} between E_c = –0.320 V and the E_a anodic limit. At E_a the potential was held for a time τ = 60 min, then the cathodic scan started. *Dashed line*: E_a = 0.645 V; *full line*: E_a = 0.685 V. On the *top* voltammogram is simultaneously recorded the same δi vs. E plot for E_a = 0.685 V. Solution pH 9.2

On the other hand, δi rises during the anodic scan for potentials higher than 0.6 V; after attaining E_a, δi still increases but at a lower rate. For times τ higher than 60 min, more stable δi values are attained. During the cathodic scan a further increase in the δi response is observed in all four experiments. In particular, the one carried out in pH 7.4 solution with E_a = 0.645 V gives the highest δi signal. Further on, the δi vs. E response declines under E = 0.35 V.

For thin films the simplest modelling assumes the photocurrent as proportional to the absorption coefficient, k, and to the thickness, d. However, the accumulation of charge at boundaries and traps may lead to more complex dependencies [4, 7, 14, 15]. The experiment made at pH 7.4 and E_a = 0.685 V shows a $\delta i/E$ peak between 0.85 V and 0.50 V. Ellipsometric measurements demonstrate that this peak and the δi augmentation during the cathodic scan do not correspond to changes in the film thickness and may be related to variations in the carrier number, the space charge and bias potential. In contrast, the progressive δi declines obtained under 0.35 V are certainly related to decreasing thickness.

The Δ and ψ parameters measured for different pH solutions and different E_a potentials are plotted in Fig. 2. The highest decrease in Δ is observed at pH 9 and E_a = 0.685 V. On the other hand, an opposite effect at pH 7.4 is observed when the potential E_a rises, resulting in a higher decrease in Δ for the lower potential of E_a = 0.645 V.

A comparison between the ellipsometric experimental results and calculations considering the growth of the passive layers allows identification of the processes taking place in different potential regions [5]. The decrease in Δ (at quasi-constant ψ) may be considered as a measure of the thickness increase of the compact passive cuprous layer formed at the metal/electrolyte interface. The experiment shown in Fig. 2 verifies the reversible (no kinetics implied) formation and reduction of this inner passive layer. The changes in the Δ/ψ values measured after reduction are close to the initial values corresponding to the bare surface. The change in Δ/ψ is small in comparison with that previously observed at E_a; note the higher sensitivity in the ψ scale in relation to that of Δ. This irreversible small increase in

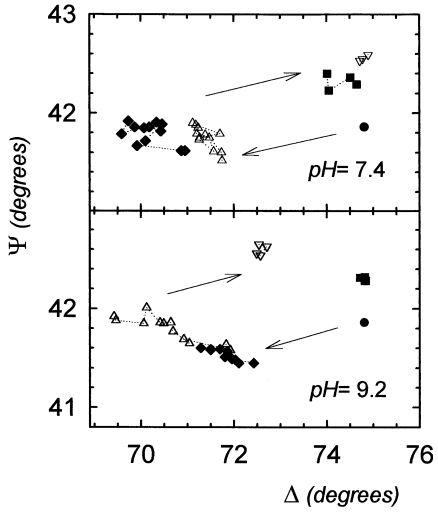

Fig. 2 Δ/ψ plot corresponding to Fig. 1. *Filled diamonds*: $E_a = 0.645$ V during $\tau = 60$ min; *filled squares*: after reduction at $E_c = -0.32$ V. *Down open triangles*: $E_a = 0.685$ V during $\tau = 60$ min; *up open triangles*: after reduction at –0.32 V. *Filled circles*: bare metal. Incident light $\lambda = 580$ nm

ψ obtained after reduction may be related to the formation of an outer hydrated Cu(II) layer [4, 5, 6, 7]. Some part of this layer may develop simultaneously with the compact layer. Nevertheless, the highest growth of the outer layer occurs during the reduction process.

In previous work [5] it was demonstrated that over 0.48 V the compact cuprous layer thickness grows proportionally to the anodic potential. This growth at pH 9.0 attains a limit thickness at about 0.650 V. This effect was related to the adsorption of Cu(II) ions on the cuprous oxide layer in contact with the electrolyte. The inner cuprous passive layer may change the number of carriers or cationic defects, depending on the ionic exchanges at both the metal/oxide and oxide/electrolyte interfaces. An increase in the cationic defects without any change in thickness was suggested by the increase in the UV optical absorption measured during the cathodic polarization of the oxide [4, 5, 6, 7]. This increase may be related to the reduction of a few Cu(I) ions to metallic copper at the metal/oxide interface.

The higher $\delta\Delta$ observed at pH 7.4 and $E_a = 0.645$ V (Fig. 2) indicates a thicker and/or a more dense passive cuprous layer than at 0.685 V. In contrast, the thickness at pH 9.0 increases for increasing times and increasing potentials E_a. The Δ/ψ values measured at $E_c = -0.312$ V, after holding at E_a the potential during a time $\tau = 65$ min, are different from those corresponding to the freshly polished electrode. Figure 2 shows, after reduction at $E_c = -0.312$ V, an increase in ψ (about 0.5°) and values of Δ similar to those of the bare surface. Theoretical simulations show that this effect does not indicate a change in roughness. Instead, it agrees with the growth of an external hydrated oxide layer [4, 5, 6, 7]. The decrease in the pH produces more porous layers; the higher porosity may be related to an increase in the adsorbed amount of Cu(II) and this effect increases on applying more anodic potentials. The calculated thicknesses d are shown in Table 1. The addition of sulfate or carbonate ions has different effects, depending on the anodic potential [4]. On the other hand, similar Δ/ψ values occur in the presence or absence of either sulfate or carbonate ions for the oxide layers formed in pH 9.2 solutions or at pH 7.4 when a high sweep rate ($v \approx 1$ V s^{-1}) is used.

EIS data

Figure 3 shows Nyquist plots of a film formed at 0.645 V (a, a′) and at 0.685 V (b, b′) during 1 h in different borate solutions at pH 7.4. The impedance diagram exhibits at high frequencies a slightly distorted capacitive semicircle (a′, b′) followed at intermediate frequencies by a linear behaviour and at low frequencies by another not completely defined contribution (a, b). The time constant at higher frequencies could be related to the electronic properties of the Cu_2O film formed and the time constant at intermediate and low frequencies should be associated with oxygen vacancy diffusion and strongly adsorbed intermediates. At pH 7.4 and at the same E_a values, lower real parts of the impedance were found when carbonate or sulfate anions are present. On the other hand, as the pH increased a rate enhancement of the processes associated with all the time constants was observed (Fig. 4).

Table 1 Ellipsometric thickness, d, charge carrier concentration, N_{SC}, and flatband potential, E_{FB}, determined from the linear portions of the Mott-Schottky plots shown in Figs. 5, 6, 7

Solution	E_a (mV)	d (nm)	E_{FB1} (V)	10^{-18} N_{SC1} (cm^{-3})	E_{FB2} (V)	10^{-18} N_{SC2} (cm^{-3})
pH 9	645	10	–	–	–	470
BO_3^{3-}	685	11	0.360	4.8	0.660	4.0
pH 7	645	29	0.405	1900	0.630	820
BO_3^{3-}	685	35	0.428	20	0.586	29
pH 7	645	15	0.410	400	0.595	590
CO_3^{2-}	685	30	0.390	270	0.640	190
pH 7	645	18	0.394	120	0.625	110
SO_4^{2-}	685	40	0.355	290	–	–
			E_{rev} (mV)		E_{rev} (mV)	
Cu/Cu_2O			0.471		–	
Cu/CuO			–		0.570	
Cu/CuO_{Hyd}			–		0.609	

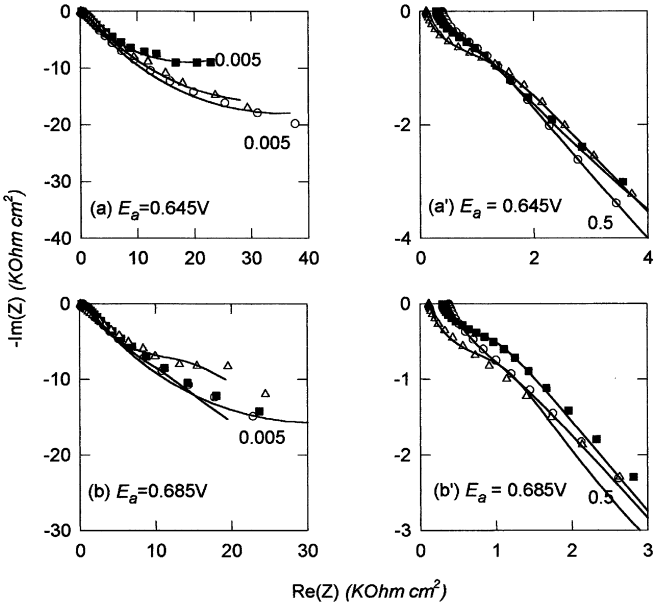

Fig. 3 Nyquist plots of Cu_2O films formed at $E_a = 0.645$ V (**a**, **a′**) and $E_a = 0.685$ V (**b**, **b′**) on copper in borate solution (*open circles*); *filled squares*: borate with addition of 3.5 mM Na_2CO_3; *up open triangles*: with addition of 8 mM Na_2SO_4. **a′**, **b′** High-frequency range. *Full lines* show the simulated data pH 7.4

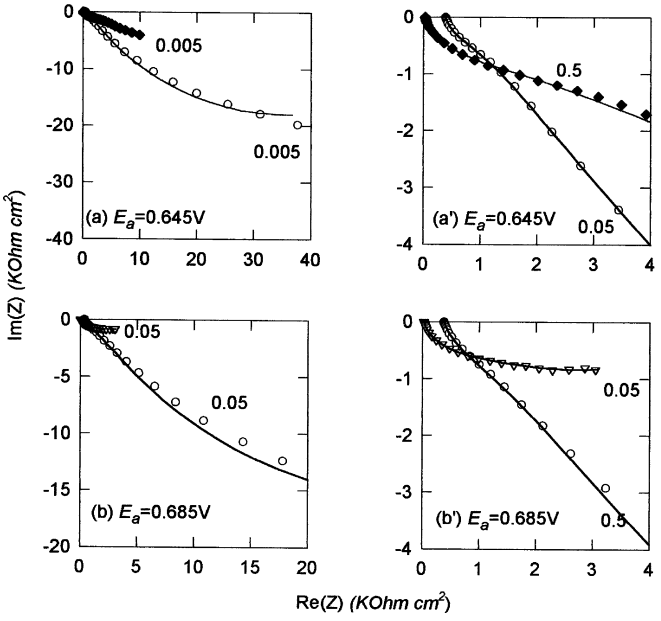

Fig. 4 Nyquist plots of Cu_2O films formed on copper in borate solution at 0.645 V (**a**, **a′**): *open circles*: pH 7.4; *filled diamonds*: pH 9.2; and at 0.685 V (**b**, **b′**): *open circles*: pH 7.4; *open down triangles*: pH 9.2. **a′**, **b′** High-frequencies range. *Full lines* show the simulated data

All the impedance experimental data can be well described by the following transfer function:

$$Z(j\omega) = R_\Omega + \frac{1}{[\mathrm{CPE}] + (R_t + Z')^{-1}} \quad (1)$$

where $\omega = 2\pi f$. The high-frequency limit R_Ω corresponds to the ohmic resistance of the electrolyte, whereas [CPE] denotes the constant phase element given by $[\mathrm{CPE}] = [C(j\omega)^\alpha]^{-1}$; C is the high-frequency capacitance, α takes into account the distribution of the time constants due to surface inhomogeneities, R_t is the charge transfer resistance associated with the couple Cu/Cu_2O and Z' corresponds to a R_aC_a time response with a second constant phase element $\alpha_a \approx 0.5 \pm 0.1$. This equivalent circuit corresponds to an electrochemical reaction with a strongly adsorbed intermediate [16]. However, the fitted values obtained for the coefficient α_a could be associated with the presence of an additional finite-length diffusion process:

$$Z_w = R_{DO}(jS)^{-1/2}\tanh(jS)^{-1/2} \quad (2)$$

where the diffusion resistance R_{DO} is the limit of $Z_w(j\omega)$ at $\omega \to 0$ and the parameter $S = d^2(\omega/D)$, D being the diffusion coefficient. This diffusion process probably occurs in the barrier part of the anodic film. This fact was mentioned also by Bojinov et al. [17].

A good agreement is obtained between the experimental results and the simulated data by using non-linear least-square fit routines and a transfer function similar to that reported by Metikos-Hukovic et al. [18] (Figs. 3 and 4). This includes Z_w in series with R_a in Eq. 2. Using this transfer function the α_a value result is close to 1. The values of C and R_t, determined from the optimum fit procedure, are, at pH 7.4, $C = 16 \pm 5$ μF cm^{-2} and $\alpha = 0.84 \pm 0.05$, while the values of R_t are in the range $405 < R_t < 1050$ Ω cm^2, for borax solution and borax with either added carbonate or sulfate ion. At pH 9.2 the R_t values are $R_t = 815$ and 940 Ω cm^2 at $E_a = 685$ and 645 mV, respectively, and lower capacitance values, $C \approx 18$ and 10 μF cm^{-2} and $\alpha \approx 1$, are obtained. The lower capacitance values are typical for a metal covered with a passive film [19, 20] and may be considered as the series combination of the film (C_{film}) and Helmholtz layer (C_H) capacitances. The potential dependence of the capacitance indicates either insulating or semiconducting properties of the passive films. On the other hand, the α values, which are higher than those corresponding to the lower pH given above, allow us to assume a more compact structure for the passive films formed at pH 9.2.

The analysis of the impedance parameters associated with the time constant contributions at intermediate and low frequencies indicates a complex process and the analysis is difficult because there are overlapping constants [16, 18]. However, from the fitting it is possible in some cases to calculate approximate values of the diffusion coefficient using the film thickness (d) estimated from ellipsometric experiments [4, 5, 6, 7]. The D values (10^{-14}–10^{-15} cm^2 s^{-1}) are in good agreement with those reported for diffusion of ions in a copper film [17, 18]. More work is in progress to improve and correlate the low-frequency response involving several time constants with the layer structure [4, 5, 6, 7, 17, 18, 19].

The calculated capacitances C associated with the loop at high frequencies have lower values than typical C_H values [21] and could be assigned to the space-charge capacitance C_{SC} of a semiconducting film [22].

At sufficiently high frequencies the transfer function (Eq. 1) can be approximated by:

$$Z(j\omega) = R_\Omega + (j\omega C)^{-1} \quad (3)$$

To estimate the capacitance C_{SC} of the oxide films, the C values calculated using non-linear least-square fit routines were corrected for the contribution from the capacitance of the Helmholtz layer [13]. Assuming a conservative constant value $C_H = 25\ \mu F\ cm^{-2}$, C_{SC} can be estimated according to:

$$C^{-1} = C_{SC}^{-1} + C_H^{-1} \quad (4)$$

Under these circumstances, the potential dependence of C_{SC} should be obtained from the well-known Mott-Schottky relation [22, 23, 24]:

$$C_{SC}^{-2} = (2/eN_{SC}\varepsilon\varepsilon_0)[-E + E_{FB} - (kT/e)] \quad (5)$$

where N_{SC} denotes the carrier concentration and E_{FB} is the flat band potential of the oxide. All the other symbols have their usual meanings.

The Mott-Schottky plots give two relatively well-defined linear portions with both positive and negative slopes (Figs. 5, 6, 7). The values of N_{SC} and E_{FB} obtained from the linear portion of the plots are summarized in Table 1. The calculated number of carriers seems to be similar in the lower or high potential region. On the other hand, there is a correlation between the C^{-2} vs. E slope and the α vs. E dependencies. Positive and negative α vs. E relationships are related to positive and negative C^{-2} vs. E slopes, respectively. This indicates that a positive slope results in a potential region where the oxide layer tends to be more homogeneous, while a negative slope is associated with an increase in the partial porosity or number of defects. This change in the α value does not indicate a change in the thickness of the cuprous layer. Previous results show that the semiconductor p-type behaviour was related to an interfacial

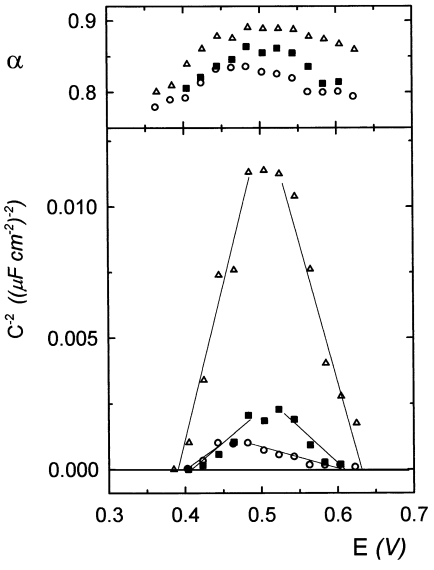

Fig. 6 Mott-Schottky plots, C_{SC}^{-2} vs. E, of the oxide formed at pH 7.4 and $E_a = 0.645$ V. *Open circles*: borate solution; *filled squares*: with addition of 3.5 mM Na_2CO_3; *open up triangles*: with addition of 8 mM Na_2SO_4

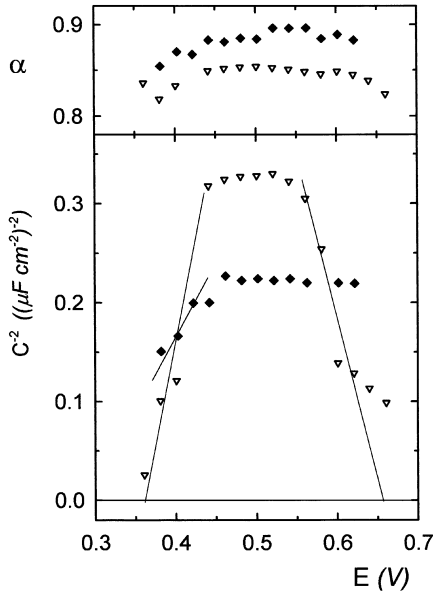

Fig. 5 Mott-Schottky plots, C_{SC}^{-2} vs. E, of the oxide formed at pH 9.2. *Filled diamonds*: $E_a = 0.645$ V; *open down triangles*: $E_a = 0.685$ V

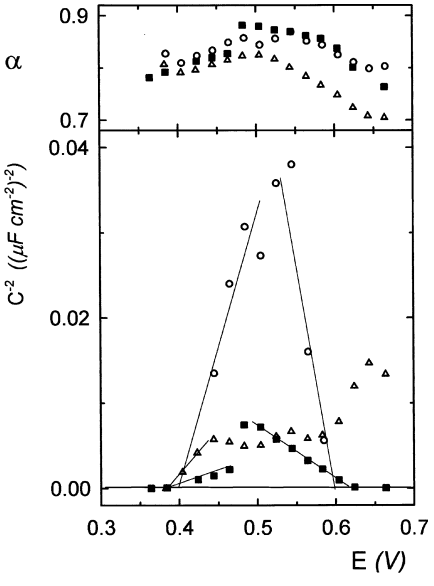

Fig. 7 Mott-Schottky plots, C_{SC}^{-2} vs. E, of the oxide formed at pH 7.4 and $E_a = 0.685$ V. *Open circles*: borate solution; *filled squares*: with addition of 3.5 mM Na_2CO_3; *open up triangles*: with addition of 8 mM Na_2SO_4

condition that tends to produce cationic defects, while n-type behaviour was observed for decreasing cationic defects [7]. All the present experiments show p-type behaviour and result in either positive or negative C^{-2} vs. E slopes, corresponding to the Cu/Cu_2O or Cu/CuO flat band (FB) potential region, respectively. The number of charge carriers calculated from both slopes are very similar for each one of the whole set of experiments. The small drift in the calculated constant phase element [CPE] indicates a progressive compactness of the Cu_2O layer in the region dominated by the Cu/CuO FB potential and a decrease in compactness in the Cu_2O/Cu FB potential region. This change occurs without changes detected in the ellipsometric parameters and is probably related to a small increase or a decrease in the formation of either inter-grain or surface cation defect domains in the Cu_2O layer.

The highest α values result at pH 9.2 and $E_a = 0.645$ V for the insulating oxide. At pH 7.4, lower α values are calculated. These results agree with the higher optical indices measured at pH 9.2 relative to those measured at pH 7.4, indicating a lower compactness of the oxide at the lower pH. In borate solution, N_{SC} values strongly decrease at $E_a = 0.685$ V for both pH values. Furthermore, the number of carriers depends on the presence of sulfate or carbonate ions. For the oxide formed at $v = 0.5$ mV s^{-1} in solutions of pH 7.4 the N_{SC} values decrease in the presence of sulfate and carbonate ions at $E_a = 0.645$ but increase at $E_a = 0.685$ V. However, for the layers formed at a high sweep rate ($v \approx 1$ V s^{-1}), or in solutions of pH 9.2, the calculated N_{SC} values are practically independent of the presence of sulfate and carbonate ions in the electrolyte. This indicates the co-precipitation or the incorporation of these ions at low growth rate conditions in the less compact layers.

Conclusions

Significant variations in the optical and dielectric properties of the cuprous layer are detected in the potential region between the Cu/Cu_2O and Cu/ CuO FB potentials. Photocurrent-potential profiles depend on the oxide layer growth potential E_a and on the pH. The double peaks obtained in the $\delta i/E$ negative-going sweep are related to variations in the carrier number, the space charge and bias potential in the cathodically polarized oxide. The calculated number of charge carriers, N_{SC}, of the cuprous oxide are very dependent on the applied E_a and on the electrolyte composition. However, the N_{SC} corresponding to each of the layers are similar for the cathodically polarized film relative to either the Cu/CuO or the Cu/Cu_2O FB potential.

Acknowledgements This research project was financially supported by the "Comisión de Investigaciones Científicas de la Provincia de Buenos Aires", the "Consejo Nacional de Investigaciones Científicas y Técnicas", the "Universidad Nacional de La Plata" and the "Fundación Antorchas". Part of the equipment used in the experimental work was provided by DAAD. The authors thank Dr. M. Miranda-Hernandez for fruitful discussions during the EIS 2001, 5th Int. Sym. on Electrochem. Impedance Spectr., Marilleva (TN), Italy, 17–22 June 2001.

References

1. Rosales B, Vera R, Moriena G (1999) Corros Sci 41:625
2. Vera R, Layan G, Gardiazabal JI (1995) Bol Soc Chil Quim 40:149
3. Maurice V, Strehblow HG, Marcus P (1999) J Electrochem Soc 146:524
4. Zerbino JO, Tapia C, Lezna RO (2000) IOM Commun 28:225
5. Zerbino JO, de Mele MFL (1997) J Appl Electrochem 27:335
6. de Mele MFL, Viera MR, Zerbino JO (1997) J Appl Electrochem 27:396
7. Zerbino JO (1999) Electrochim Acta 45:819
8. Di Quarto F, Piazza S, Sunseri C (1985) Electrochim Acta 30:315
9. Smith M, Gotovac V, Aljinovic Lj, Lucic-Lavcevic M (1995) Surf Sci 335:171
10. Sutter EM, Fiaud C, Lincot D (1993) Electrochim Acta 38:1471
11. Zhou GD, Shao H, Loo BH (1997) J Electroanal Chem 421:129
12. Wieder H, Czanderna AW (1966) J Appl Phys 37:184
13. Gassa LM, Mishima HT, Lopez de Mishima BA, Vilche JR (1997) Electrochim Acta 42:1717
14. Gerischer H (1989) Corros Sci 29:257
15. Schwartz DT, Muller RH (1991) Surf Sci 248:349
16. Raistrick ID, Ross Macdonald J, Franceschetti DR (1987) In: Ross Macdonald J (ed) Impedance spectroscopy. Wiley, New York, pp 75, 95
17. Bojinov M, Hilden J, Laitinen T, Mäkelä K, Piipo J, Saario T, Hinttala J (2000) Passivity of metals and semiconductors. In: Ives MB, Luo JL, Rodda J (eds). The Electrochemical Society, Pennington, NJ, pp 555–560
18. Metikos-Hukovic M, Babic R, Marinovic A (1998) J Electrochem Soc 145:4045
19. Simoes AMP, Ferreira MGS, Randot B, Da Cunha Belo M (1990) J Electrochem Soc 137:82
20. Gomes WP, Vanmaekelbergh D (1996) Electrochim Acta 41:967
21. Burbank J, Simon AC, Willihnganz E (1971) In: Delahay P, Tobias CW (eds) Advances in electrochemistry and electrochemical engineering, vol 8. Wiley, New York, p 158
22. Morrison SR (1984) Electrochemistry at semiconductor and oxidized metal electrodes. Plenum, New York
23. Schottky NF (1942) Z Phys 181:539
24. Mott NF (1939) Proc R Soc London Ser A 171:27